**archives**
**of thermodynamics**
Vol. **33**(2012), No. 1, 139–152
DOI: 10.2478/v10173-012-0007-y

# Model of heat transfer in the stagnation point of rapidly evaporating microjet

**DARIUSZ MIKIELEWICZ**[1]*
**TOMASZ MUSZYŃSKI**[1]
**JAROSŁAW MIKIELEWICZ**[2]

[1] Gdansk University of Technology, Faculty of Mechanical Engineering, Narutowicza 12, 80-233 Gdansk, Poland

[2] The Szewalski Institute of Fluid Flow Machinery of Polish Academy of Sciences, Fiszera 14 80-231 Gdansk, Poland

**Abstract** The paper presents investigation into the single water microjet surface cooling producing evaporating film. Reported tests were conducted under steady state conditions. Experiments were conducted using the nozzle size of 70 and 100 $\mu$m respectively. In the course of investigations obtained were experimental relations between heat flux and wall superheating. It was proved that the phenomenon is similar to that of pool boiling but the boiling curves are showing a smaller value of critical heat flux (CHF) that the stagnant pool boiling. Values of CHF are also reduced with decreasing liquid subcooling. Theoretical model of surface cooling by evaporating microjet impingement in the stagnation point was described theoreticaly. Results of experiments were compared with predictions by the model showing a good consistency.

**Keywords:** Microjet cooling; Surface cooling, CHF

## Nomenclature

| | | |
|---|---|---|
| $c_p$ | – | specific heat, J/kg K |
| $D$ | – | jet diameter, m |
| $G$ | – | mass velocity, kg/m$^2$s |

*Corresponding author. E-mail address: Dariusz.Mikielewicz@pg.gda.pl

$g$ – acceleration due to gravity, m/s$^2$
$h$ – specific enthalpy, J/kg, height in Fig. 4
$H$ – jet suspension over surface of impingement, m
Ja – Jacob number
$\dot{m}$ – mass flux, kg/s
Nu – Nusselt number
$p$ – pressure, Pa
Pr – Prandtl number
$q$ – heat flux, W/m$^2$
$R$ – radiuis of liquid film evaporation, m
Re – Reynolds number
$T$ – temperature, K
$V, u$ – velocity components, m/s

**Greek symbols**

$\alpha$ – heat transfer coefficient, W/m$^2$K
$\delta$ – film thickness, m
$\lambda$ – thermal conductivity, W/mK
$\rho$ – density, kg/m$^3$
$\tau$ – time, s
$\sigma$ – surface tension, N/m
$\zeta$ – contraction factor

**Subscripts**

$cr$ – critical
$exp$ – experimental
$d$ – dynamic
$h$ – hydrostatic
$l$ – liquid
$SAT$ – saturation conditions
$sub$ – subcooling
$t$ – total
$th$ – theoretical
$w$ – wall parameter
$v$ – vapour
0 – inlet to nozzle

# 1 Introduction

Accurate control of cooling parameters is required in ever wider range of technical applications. It is known that reducing the dimensions of the size of the nozzle leads to increase in the economy of cooling and improves its quality[1–6]. Present study describes research related to the design and construction of the nozzles and microjet study, which may be applied in many technical applications such as metallurgy, electronics, etc.

Using liquids such as water, boiling is likely to occur when the surface temperature exceeds the coolant saturation temperature. Boiling is associated with large rates of heat transfer because of the latent heat of evaporation and because of the enhancement of the level of turbulence between the liquid and the solid surface. This enhancement is due to the mixing action associated with the cyclic nucleation, growth and departure or collapse of vapour bubbles on the surface. In the case of flow boiling, such as boiling under impinging jets, the interaction between the bubble dynamics and the jet hydrodynamics has significant effect on the rate of heat transfer. The common approach used to determine the rate of boiling heat transfer is by using a set of empirical equations that correlate the value of the surface heat flux or the heat transfer coefficient with the fluid properties, surface conditions and flow conditions.

These correlations do not provide much insight into the underlying physical mechanisms involved in the boiling heat transfer problem. The alternative approach is to use mechanistic models. Generally speaking, a mechanistic model is usually based on the concept of surface heat flux partitioning. In such case assumption is made that the surface heat flux comprises of multiple components. These components usually are the amount of heat used for direct evaporation to generate the bubbles, the amount of heat transferred through transient conduction to the liquid replacing the departing bubbles and the amount of heat transferred through the enhanced convection due to the wakes generated by the emerging bubbles into the liquid. All mechanistic models of boiling heat transfer rely on experimentally developed relations or sub-models. These relations are used to correlate between the bubble departure diameter and release frequency and the other flow and surface parameters. There have been a number of mechanistic models developed for the case of pool boiling and for the case of parallel flow boiling. In the latter case, the boiling heat transfer phenomenon is more complicated due to the strong coupling between the flow, the thermal field, and bubble dynamics.

None of the existing mechanistic models considered the case of boiling heat transfer under impinging jets, where the flow field is quite different from the case of parallel flow. Under an impinging jet, the velocity is normal to the surface at the stagnation zone. Downstream of the stagnation zone there is a parallel flow region where the hydrodynamic and thermal boundary layers are developing. One of the rare examples of modelling the heat transfer in stagnation point is the study due to Omar *et al.* [8]. The

model predicts the total wall heat flux in the stagnation region of a free planar jet impinging on the flat surface. The model utilizes the concept of additional diffusion due to bubble-induced mixing. Authors accomplished a set of experiments in order to develop the required correlation between the additional diffusivity and the jet velocity, the degree of subcooling, and the degree of surface superheat. Model predictions give reasonable accuracy with experiments.

Main objective of this paper is to investigate the physical phenomena occurring on solid surfaces upon impingement of the single water microjet. Intense heat transfer in the impact zone of microjet has been examined and described with precise measurements of thermal and flow conditions of microjets. Obtained database of experimental data with analytical solutions and numerical computer simulation allows the rational design and calculation of microjet modules and optimum performance of these modules for various industrial applications.

The basis of microjet technology is to produce laminar jets which when impinging the surface have a very high kinetic energy at the stagnation point. Boundary layer is not formed in those conditions, while the area of film cooling has a very high turbulence resulting from a very high heat transfer coefficient. Applied technology of jet production can result with the jet size ranging from 20 to 500 $\mu$m in breadth and from 20 to 100 $\mu$m in width. The paper presents the investigation of a single water microjet cooling forming an evaporating liquid film on the impingement surface. Examined is the influence of liquid subcooling on the extent of the critical heat flux. Tests were conducted under steady state conditions. Developed also has been a theoretical model of surface cooling by evaporating microjet impinging in the stagnation point, where the highest heat transfer coefficient occurs.

## 2 Experimental facility

Present study shows the results of steady state heat transfer experiments, conducted for nucleate boiling regime to obtain boiling curves. Studies enable also determination of critical boiling heat fluxes. Figure 1 shows the schematic diagram of the test section. It consists of the probe, water supplying system, the measuring devices and DC power supply. Distilled water is fed to the nozzle from a water tank, which also serves as the pressure accumulator. The water pressure in the test section is raised by air

compressor. Desired water flow rate is obtained by sustaining the constant pressure of water with a proper use of flow control valve. In order to reduce the pressure drop necessary to create a steady laminar jet the nozzle was 2 mm long. Volumetric water flow rate is measured at inlet and outlet from the cooling chamber with a graduated flask.

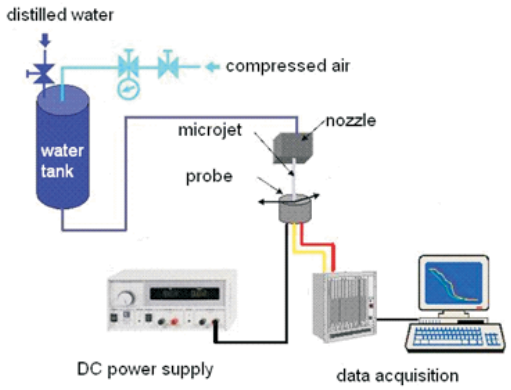


Figure 1. Schematic diagram of test section.

The water tank is also fitted with preliminary water heater, which allows to adjust water jet temperature for cooling, i.e. control of liquid subcooling. The distance between the nozzle exit and the cooled surface is fixed at the distance of H = 25 mm. Figure 2 shows the cross-section of the probe. The cooled surface is the copper cone with truncated top with upper side diameter of 10 mm and 20 mm height. Water impingement surface

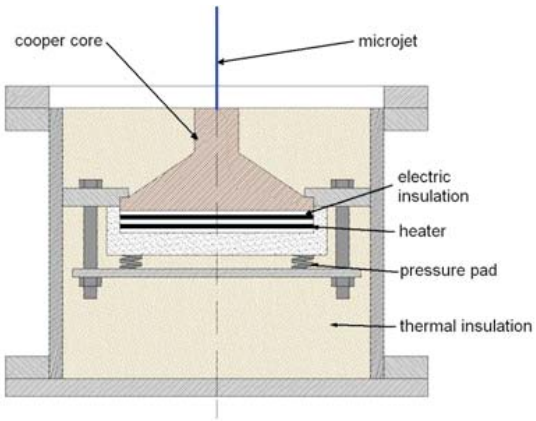


Figure 2. Cross-section of the probe.

is silver-plated, in order to prevent high temperature erosion. The radial distribution of surface temperature is determined with the aid of five T-type thermocouples, created from embedding 50 $\mu$m thick constantan wire to the copper core. Heat is supplied by a kanthal heater mounted at the bottom of the core. The whole set is thermally insulated and placed in the casing. Heater is powered by a DC power supply and the total power input is determined by measuring current intensity and voltage.

Additional four K-type thermocouples are attached in the copper rod vertical axis. These thermocouples measure axial temperature gradient at the core of a heating block and control temperature of the heater. They are connected to the National Instruments data acquisition set. The signal from thermocouples was processed with the aid of the LabVIEW application. Heater operating power values are precisely controlled and measured. The applied power losses through conduction into the insulation and radiation to the surroundings are accurately calculated and accounted for in all tests. Data are taken from a steady state measuring points in order to exclude heat capacity of the installation.

Nozzle construction allows to modify its dimensions. Two nozzle hydraulic diameters were used namely 0.101 and 0.71 mm. As mentioned earlier experiments were conducted for the spacing of 25 mm between the nozzle exit and impinging surface. Because of the limited power supply, the low water mass flux values were used in order to obtain fully developed boiling and critical heat flux. Measurements were performed in three series with varying water subcooling.

## 3 Theoretical model

In the analysis of accomplished experiments the simple theoretical model of impinging and evaporating liquid microjet is presented. Proposed is the model of heat transfer in the stagnation zone, where liquid rapidly evaporates due to contact with the hot surface. The model is developed on the basis of known pressure difference between the nozzle exit and the stagnation point. As a result of evaporation of impinging jet, there is formed a vapour blanket on the surface. The dynamic pressure is the way in which the nozzle interacts with the surface, given by $\Delta p_d = \rho u_D^2/2$, where $u_D$ is the velocity at nozzle outlet. In the analysis considered also could be the capillary effect $\Delta p_{cap} = \sigma/D$ (with $D$ being the nozzle diameter and $\sigma$ the surface tension) and the hydrostatic pressure drop $\Delta p_h = (\rho_l - \rho_v)\, gH$

(where $H$ denotes the jet distance from the surface). The latter two have however been omitted in the present study as they have been regarded as of secondary importance. The total pressure acting on the surface yields:

$$\Delta p_t = \Delta p_d + \Delta p_{cap} + \Delta p_h \ . \tag{1}$$

The schematic of rapidly evaporating microjet is presented in Fig. 3. The radius, $R$, on which the spreading of liquid film is taking place can be determined from the energy balance on the element of the cooled plate, which reads:

$$q\pi R^2 = \dot{m}_l \left[h_{lv} + c_p \left(T_{SAT} - T_0\right)\right] \ , \tag{2}$$

where $q$ is the wall heat flux, $c_p$ is the specific heat at constant pressure, $\dot{m}_l$ is the mass flowrate of liquid, $h_{lv}$ is the latent heat of evaporation, $T_{SAT}$ is the saturation temperature, $T_0$ is the temperature at nozzle outlet.

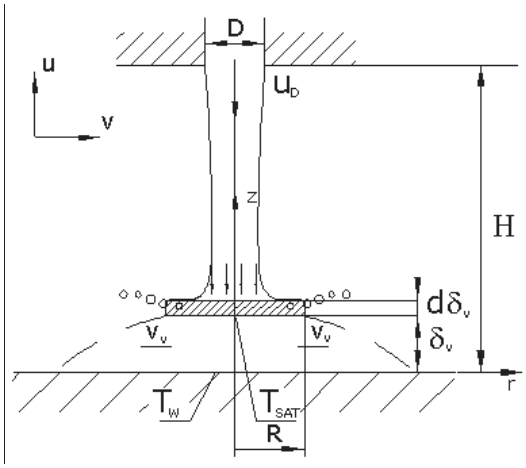


Figure 3. Scheme of rapidly evaporating microjet.

From (2) the radius of impingement can be found from expression:

$$R = \sqrt{\frac{\dot{m}_l(h_{lv} + c_p \Delta T)}{\pi q}} \ , \tag{3}$$

where $\Delta T$ is the difference between saturation and nozzle outlet temperatures.

The applicability for further calculations of the radius obtained from Eq. (3) has also been confirmed experimentally in the course of authors

own experiment [9]. In that study values or the range of cooling of the surface, obtained from (3) showed a very good consistency with experimental evidence. Substituting into that equation values of water properties at atmospheric pressure and temperature 20 °C ($c_p$ = 4184.3 J/kg K, $h_{lv}$ = 2256.4 kJ/kg, and $\Delta T$ = 80 K) the obtained radius of cooling was equal to 2.87 mm, which agreed very well with experimental finding for that case when the mass flow rate was $3\times10^{-5}$ kg/s and heat flux $q = 3.0$ MW/m$^2$.

In the analysis of the evaporating jet the following assumptions were made:

- only a dynamic part of pressure difference in (1) is considered in the model,
- liquid temperature on the radius of evaporation $R$ is higher than saturation temperature.

The mass balance on evaporation surface yields:

$$dm_l = \pi R^2 d\delta \rho_l = dm_v = 2\pi R \delta_v \rho_v V_v d\tau \ , \tag{4}$$

where $\delta$ is the film thickness, $V_v$ is the vapour velocity, $d\tau$ is the time interval.
Equation (4) enables to determine the expression for estimation of the film thickness, which in rearranged form reads:

$$\dot{m}_l = \frac{dm_l}{d\tau} = 2\pi R \delta_v \rho_v V_v \ . \tag{5}$$

In order to solve Eq. (5) we must provide the means for calculation of vapour velocity. That can be done relying of the concept of liquid outflow through a small hole. In our approach we assume that the radial vapour motion from the stagnation point can be modeled in a similar way. It is assumed in our approach that vapour which is formed as a result of impingement forms a cylinder with the base corresponding to the nozzle diameter, as shown in Fig. 3. Such motion can be modeled as flow of vapour from the side wall of the cylinder of the size $\pi D\delta$, where $D$ is the jet diameter and $\delta$ is the film thickness by analogy to the outflow from the tank through a small hole. Such problem, can be solved as sketched in Fig. 4, by consideration of the Bernouli equation:

$$p_1 + \frac{\rho_v u_1^2}{2} + g h_1 = p_2 + \frac{\rho_v u_2^2}{2} + g h_2 \ , \tag{6}$$

where $p, u, h$ denote pressure, velocity and enthalpy at locations 1 and 2 respectively.

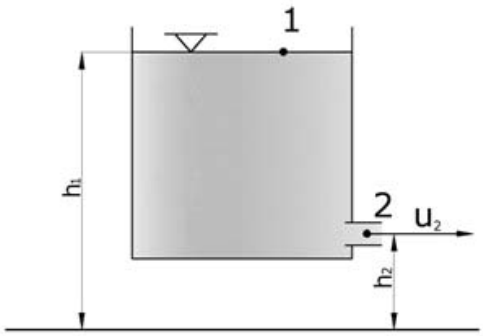


Figure 4. Outflow from the large tank through a small hole.

Solution is obtained assuming that $u_1 = 0$ and velocity at outlet is determined from the expression:

$$u_2 = \zeta \sqrt{\frac{2\Delta p}{\rho}} \,, \tag{7}$$

when $\zeta$ is the contraction coefficient and $\Delta p$ is the pressure difference $p_1 - p_2$.

In our case we are dealing with the flow of vapour coming out of the nozzle. Hence we assume that $\rho = \rho_v$. We are aware that although in the classical solution to the model velocity at state 1 is assumed zero, in our case it has a finite value which can be determined from the heat balance equation:

$$u_1 = \frac{q}{\rho_v h_{lv}} \,, \tag{8}$$

where $q$ is the heat flux and $h_{lv}$ is the latent heat of evaporation.

Equation (8) will be attempted to be included into modeling but for the time being the vapour velocity is considered as:

$$V_v = \zeta \sqrt{\frac{2\Delta p_t}{\rho_v}} \,, \tag{9}$$

where $\Delta p_t = \frac{1}{2}\rho_l u_D^2$ is the microjet dynamic pressure. Substituting vapour velocity to Eq. (5):

$$\dot{m}_l = 2\pi R \delta_v \zeta \sqrt{\rho_v \rho_l} u_D \tag{10}$$

and after describing heat transfer on cooled surface as heat transition in vapour layer $q = \frac{\lambda_v}{\delta_v}(T_W - T_{SAT})$, where $T_W$ is the wall temperature, the film thickness can be determined from the experiment:

$$\delta_v = \sqrt{\frac{\lambda_v (T_w - T_{SAT}) D}{4\zeta \sqrt{\rho_l \rho_v} u_D \left[h_{lv} + c_p (T_{SAT} - T_0)\right]}} \,. \tag{11}$$

Knowledge of film thickness allows to determine the heat transfer coefficient and hence the Nusselt number:

$$\mathrm{Nu} = \frac{\alpha\, D}{\lambda_v} = \frac{2}{\sqrt{\dfrac{\mathrm{Ja}_v}{\zeta\, \mathrm{Pr}_{lv}(1 + \mathrm{Ja}_l)}}} \,, \tag{12}$$

where the Prandtl and Jacob numbers for vapour and liquid are defined respectively as follows:

$$\mathrm{Pr}_{lv} = \frac{\nu_l}{a_{vl}} = \frac{\nu_l}{\frac{\lambda_v}{c_{pv}\sqrt{\rho_l \rho_v}}} \,, \quad \mathrm{Ja}_v = \frac{(T_W - T_{SAT})\, c_{pv}}{h_{lv}} \,, \quad \mathrm{Ja}_l = \frac{(T_{SAT} - T_0) c_{pl}}{h_{lv}} \,.$$

Some attention should be devoted to the calculation of the contraction factor present in Eq. (9). The good consistency of results is partially devoted to the fact that the contraction factor present in Eq. (9) is calculated from the formula:

$$\zeta = 2.3610^6 \mathrm{Re}^{-1.54} \left(\frac{q}{q_{cr}}\right)^{2.2} \,, \tag{13}$$

where $q_{cr}$ is the critical heat flux.

## 4 Results of calculations

Figure 5 shows the experimental results of fully developed nucleate boiling heat transfer at the stagnation zone for impinging saturated water jet using the nozzle with $D = 0.071$ mm. Heat transfer data are plotted in the form of boiling curves for different liquid mass flux. The Kutatieladze's empirical correlation for prediction of critical heat flux is also presented as a solid line to point out the similarity of the considered jet cooling to the pool boiling case of liquid. For nucleate pool boiling of water at atmospheric pressure, correlation due to Kutateladze can be simplified to [7]:

$$q_{cr} = 15.58 (T_W - T_{SAT})^{\frac{10}{3}} \left[\frac{W}{m^2}\right] \,. \tag{14}$$

A clear trend can be observed that increasing mass flux of liquid leads to the higher value of critical heat flux. The curves follow in a qualitative way the distribution of the boiling curve predicted by the equation due to Kutateladze. Higher mass fluxes also result in smaller wall superheats, however are shifted left. Figures 6 and 7 shows stagnation point heat transfer coefficients, for different liquid subcoolings. In both cases increased water inlet temperature resulted in higher heat transfer coefficients.

Figure 8 presents the stagnation point heat transfer coefficients in func-

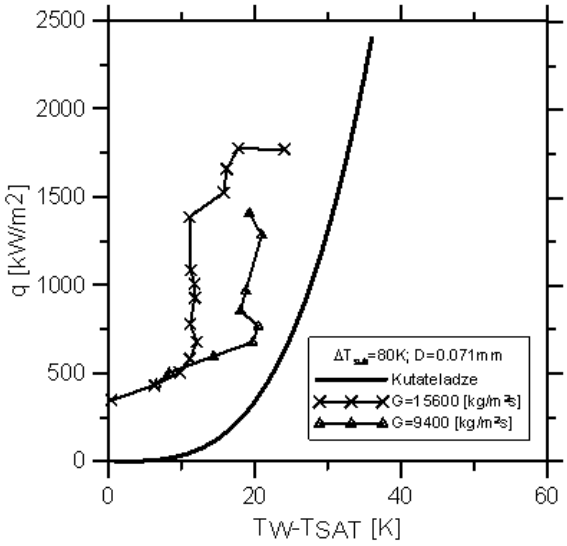


Figure 5. Nucleate boiling curves of evaporating water jet for the nozzle diameter $D =$ 0.071 mm.

tion of predicted values of heat transfer coefficient resulting from Eq. (12). Application of (13) enables calculation of heat transfer coefficients with a very reasonable accuracy. In Fig. 9 presented are distributions of experimental to theoretical Nusselt number ratio in function of wall superheating, which proves that the model (12) is capable of appropriate capturing of the trends in boiling heat transfer during impingement in the stagnation point. A trend to underpredict the heat transfer coefficient in higher wall superheat can be diminished by refinement of Eq. (13).

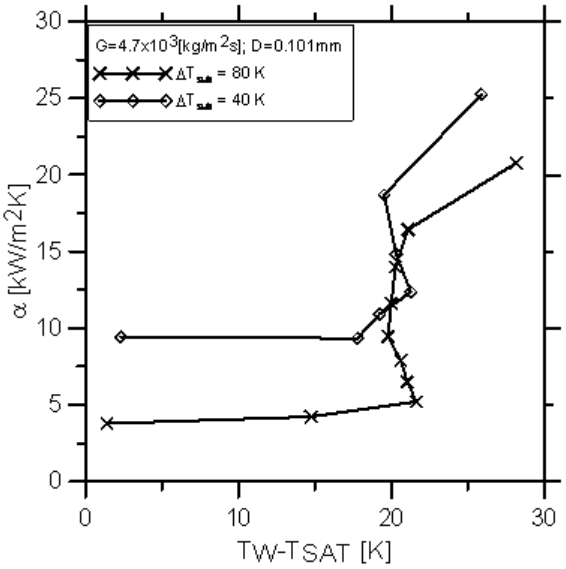


Figure 6. Nucleate boiling heat transfer coefficients of evaporating water jet for the nozzle diameter $D = 0.101$ mm.

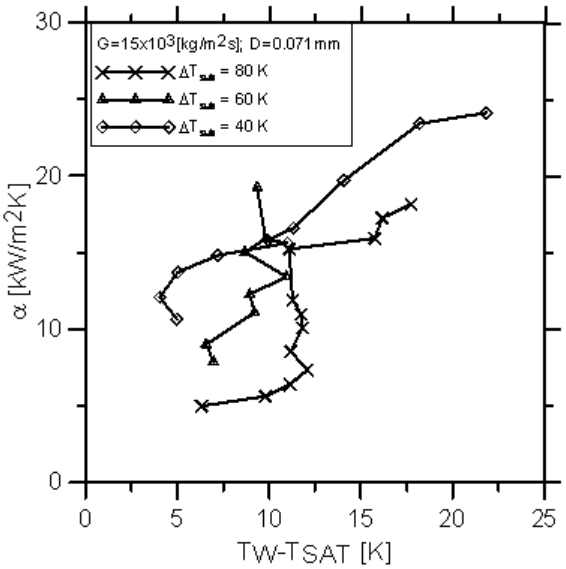


Figure 7. Nucleate boiling heat transfer coefficients of evaporating water jet for the nozzle diameter $D = 0.071$ mm.

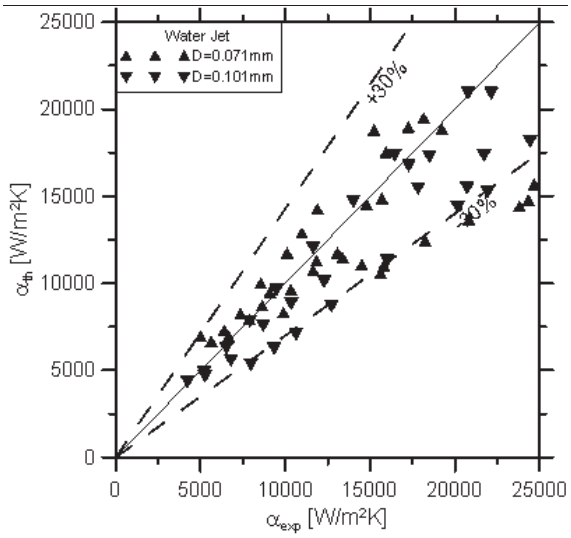


Figure 8. Relation between experimental and theoretical heat transfer coefficients calculated using Eq. (12).

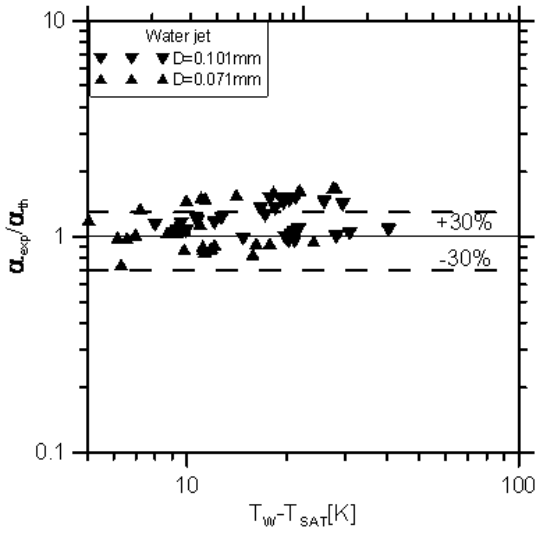


Figure 9. Relation between experimental and theoretical heat transfer coefficients in function of wall superheat.

## 5 Conclusions

In the paper presented have been theoretical and experimental studies of evaporating microjet impingement. Analytical model for calculation of the

stagnation Nusselt number was presented.

Very important issue in calculation of heat transfer in microjet cooling is calculation of the contraction factor (13). It has been found that its value varies with liquid subcooling. This is a completely new application of that factor, where no experimental evidence exists. Approach to model it presented in the paper is very tentative, however exhibiting satisfactory results. Future activities should proceed in the direction of better determination of that parameter.

**Acknowledgements** The work presented in the paper was partially funded from the Ministry for Science and Higher Education research grant R06 01103 in years 2007–2010 and H512 455240 in years 2011–2013.

*Received 4 January 2011*

## References

[1] Garimella S.V., Rice R.A.: *Confined and submerged liquid jet impingement heat-transfer*. JHT **117**(1995), 871–877.

[2] Mikielewicz D., Muszynski T.: *Experimental study of heat transfer intensification using microjets*. In: Proc. Int. Symp. on Convective Heat and Mass Transfer in Sustainable Energy, Hammamet 2009, Tunisia.

[3] Goldstein R.J., Timmers J.F.: *Visualisation of heat transfer from arrays of impinging jets*. Int. J. Heat Mass Transfer **25**(????) 1857–1868.

[4] Meyer M.T., Mudawar I.: *Single-phase and two-phase cooling with an array of rectangular jets*. Int. J. Heat Mass Transfer **49**(2006), 17–29.

[5] Sung M.K., Mudawar I.: *Single-phase and two-phase heat transfer characteristics of low temperature hybrid micro-channel/micro-jet impingement cooling module*, Int. J. Heat Mass Transfer **51**(2008), 3882–3895.

[6] San J., Lai M.: *Optimum jet-to-jet spacing of heat transfer for staggered arrays of impinging air jets*. Int. J. Heat Mass Transfer **44**(2001), 3997–4007.

[7] Liu Z.-H., Zhu Q.-Z.: *Prediction of critical heat flux for convective boiling of saturated water jet impinging on the stagnation zone*. J. Heat Transfer **124**(2002), 1125–1130.

[8] Omar A.M.T., Hamed M.S., Shoukri M.: *Modeling of nucleate boiling heat transfer under an impinging free jet*. Int. J. Heat Mass Transfer **52**(2009), 5557–5566.

[9] Plata M.: *Microjet cooling*. Doctoral seminar, Gdańsk 2007.